A COVARIANT DESCRIPTION OF THE DEUTERON AND A BUNCH OF OTHER STUFF

by

A. Student

A Thesis Submitted to the Faculty of the Department of Physics
Old Dominion University in Partial Fulfillment of the
Requirements for the Degree of

BACHELOR OF SCIENCE

PHYSICS

OLD DOMINION UNIVERSITY
June 2012

Approved by:

_____
Khan Doe (Director)

_____
Jane Roe (Member)

_____
Albert Einstein (Member)

ABSTRACT

A COVARIANT DESCRIPTION OF THE DEUTERON AND A BUNCH OF OTHER STUFF

A. Student
Old Dominion University, 2022
Director: Dr. Khan Doe

An introduction to the use of Bethe-Salpeter and quasipotential equations in the description of electron scattering from the deuteron is provided. The basic formalism and many technical issues are introduced in the context of a simple scalar theory. Results for bound-state wave functions and scattering phases shifts for a variety of quasipotential prescriptions are presented and qualitative characteristics of these solutions are discussed. The elastic form factors for the bound state in this model are calculated using the spectator or Gross equation. The calculations are then extended to account for the complexities associated with nucleon spin and results are presented for the elastic structure functions of the deuteron using the spectator equation. This calculation is shown to produce a good description of elastic electron scattering from the deuteron over the range of momentum transfers for which data are available.

ACKNOWLEDGMENTS

I would like to thank...

TABLE OF CONTENTS

LIST OF TABLES

LIST OF FIGURES

CHAPTER 1

INTRODUCTION

With the advent of CEBAF, it will become routine to probe nuclear systems with electron scattering where the energy and momentum transfers will be well in excess of the nucleon mass. Under such circumstances, the usual nonrelativistic description of the nucleus is no longer reliable. It is, therefore, necessary to develop relativistically covariant models of the nuclear system. This is a difficult task and most work has been concentrated on the two-nucleon system, although extensions to three-body systems are being studied.

There are basically three approaches to the construction of covariant models of the deuteron: relativistic Hamiltonian dynamics [1, 2], Bethe-Salpeter [3, 4, 5, 6] and related quasipotential equations [7, 8, 9, 10, 11, 12, 13, 14, 15, 16, 17, 18, 19, 20, 21], and light-cone field theory [22, 23]. The first of these concentrates on the application of Poincare invariance to Hamiltonian theories with potential-like interactions. The Bethe-Salpeter and light-cone field theories are derived from field theory, although actual applications to two-nucleon systems require the introduction of phenomenological elements. The Bethe-Salpeter equation and the related quasipotential equations are based on Feynman perturbation theory and, as such, maintain manifest Lorentz invariance. The light-cone field theory approach is based on the evolution of field theories quantized along the light-cone. Both the Hamiltonian dynamics and the light-cone field-theory focus on the "time" evolution of interacting systems and are organized such that the calculations are covariant but not necessarily manifestly covariant.

This paper focuses on the application on Bethe-Salpeter and quasipotential approaches to the modeling of the deuteron. The actual calculation of these models can become quite complex due to the spin degrees of freedom of mesons and nucleons. For this reason, it is instructive to first consider these equations in the context of a simple model containing only scalar particles. The basic structure of these equations is easily described and the calculation of bound states and scattering amplitudes is considerably less formidable. This allows the solutions to be examined for a variety of quasipotential equations. Some interesting qualitative features of these calculations

can be identified that will carry over into more realistic models. In particular, it is shown that the scattering phase shifts seem to be relatively insensitive to the choice of quasipotential equation provided that the model parameters are appropriately adjusted to obtain a bound state at a fixed mass. The spectator or Gross equation is chosen to demonstrate the problems associated with the calculation of electromagnetic current matrix elements in quasipotential models. This model is used to calculate the elastic electron scattering form factor for the scalar "deuteron" and the effects of variation of nucleon cutoffs and approximations to the single-nucleon current operator are studied.

The basic concepts introduced in the context of the scalar model are extended to cover more realistic models of two spin-$\frac{1}{2}$ nucleons interacting through the exchange of mesons with a variety of masses, spins and isospins. Some of the additional complications arising from these additional internal quantum numbers are introduced. Two interaction models are discussed and applied to the calculation of the structure functions for elastic electron scattering from the deuteron. The calculations are in good agreement with the data available for these structure functions.

CHAPTER 2

RELATIVISTIC WAVE EQUATIONS AND A LOT OF OTHER STUFF

2.1 THE BETHE-SALPETER EQUATION

It is useful to introduce a simple model for the introduction of the ideas and formalism of the Bethe-Salpeter equation. For this purpose, consider a simple field theory of two heavy scalar particles interacting by the exchange of a light scalar particle. This model allows consideration of the basic structure of the Bethe-Salpeter equation without dealing with the complication of spin and the exchange of multiple mesons as is necessary in a realistic model of the deuteron. The equations resulting from this simple analysis will be extended to include these complications in Section VI.

The Bethe-Salpeter equation [3] for a two-body system can be derived from quantum field theory and a rigorous derivation is outlined in Refs. [24, 25]. Here, simple arguments are used to suggest the form and content of the Bethe-Salpeter equation. First, consider all of the Feynman diagrams that contribute for the scattering of two heavy scalars, which can be thought of as scalar nucleons, by the exchange of a light scalar meson as represented in Fig. 1. The solid lines represent propagators for the scalar nucleons and the dashed lines represent propagators for the scalar mesons. These diagrams are intended to represent skeleton diagrams where all diagrams which represent dressings of propagators or three point vertices are subsumed into the propagators or vertices. Diagrams (1b) and (1d) are double and triple iterations of diagram (1a). Diagrams (1e) and (1f) are diagram (1c) preceded and followed by diagram (1a). This suggests a scheme for summing all of the contributions to the scattering matrix. This is done by introducing the concept of a two-particle irreducible diagram. A diagram which can not be separated into two or more diagrams by cutting just two nucleon propagators is said to be irreducible. By this definition, the diagrams (1b), (1d), (1e) and (1f) are reducible since they can be cut into two or more simple diagrams as illustrated by the dotted lines in Fig.

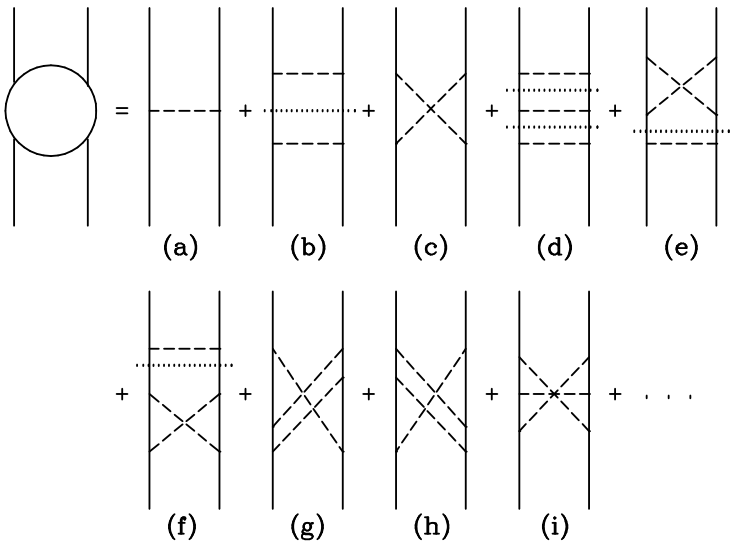

FIG. 1: Feynman diagrams representing the scattering of two heavy scalar nucleons (solid lines) by the exchange of a light scalar mesons (dashed lines. Dotted lines show two-nucleon cuts for reducing the diagrams.

1. The remaining diagrams, (1a), (1c), (1g), (1h) and (1i) are irreducible since any cut across the diagrams will cut at least one meson propagator as well as the two nucleon propagators.

If the Bethe-Salpeter interaction kernel V is defined to be the sum of all two-particle irreducible diagrams as represented by the diagrams in Fig. 2, the sum of all possible contributions to the $\mathcal{M}$ matrix can be represented diagramatically by Fig. 3. This equation treats the nucleon degrees of freedom explicitly while all of the meson degrees of freedom are contained in the interaction kernel. Standard Feynman rules can be used to obtain an integral equation for the $\mathcal{M}$ matrix. This can be represented as

$$\mathcal{M}(p',p;P) = V(p',p;P) - \int \frac{d^4k}{(2\pi)^4} V(p',k;P) G_0(k;P) \mathcal{M}(k,p;P), \qquad (1)$$

or equivalently,

$$\mathcal{M}(p',p;P) = V(p',p;P) - \int \frac{d^4k}{(2\pi)^4} \mathcal{M}(p',k;P) G_0(k;P) V(k,p,;P), \qquad (2)$$

where P is the total four-momentum of the nucleon pair, and p', k and p are the final, intermediate and initial relative four-momenta of the nucleon pair. The two-nucleon

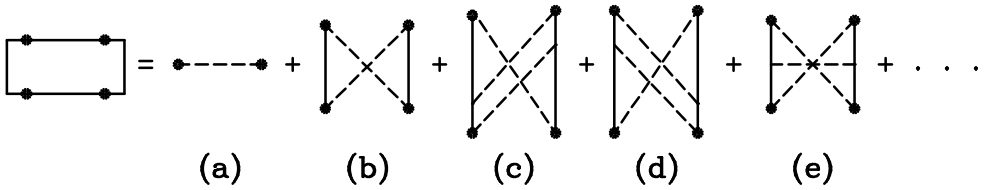

FIG. 2: Feynman diagrams representing the two-nucleon irreducible kernel.

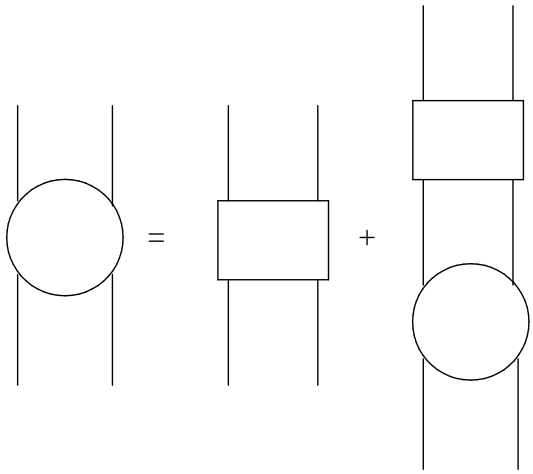

FIG. 3: Feynman diagramatical representation of the Bethe-Salpeter equation for the $\mathcal{M}$ matrix.

intermediate propagator is defined as

$$G_0(k;P) = -i\Delta_F^{(1)}(\frac{P}{2}+k,m)\Delta_F^{(2)}(\frac{P}{2}-k,m), \tag{3}$$

where

$$\Delta_F^{(i)}(p,m) = \frac{1}{p^2-m^2+i\eta} \tag{4}$$

is the propagator for particle i with mass m. Note only the pole part of the dressed single-particle progagator is retained, as is conventional in such models. The contributions from the residual part of the propagator can be included in a variety of ways, but this complication is ignored here.

The equations for the conjugate of the $\mathcal{M}$ matrix

$$\mathcal{M}^\dagger(p',p;P) = V^\dagger(p',p;P) - \int \frac{d^4k}{(2\pi)^4}\mathcal{M}^\dagger(p',k;P)G_0^\dagger(k;P)V^\dagger(k,p,;P), \tag{5}$$

and

$$\mathcal{M}^\dagger(p',p;P) = V^\dagger(p',p;P) - \int \frac{d^4k}{(2\pi)^4}V^\dagger(p',k;P)G_0^\dagger(k;P)\mathcal{M}^\dagger(k,p;P), \tag{6}$$

can be used to derive the unitarity relation for the $\mathcal{M}$ matrix

$$\begin{aligned}\mathcal{M}(p',p,;P) \quad - \quad & \mathcal{M}^\dagger(p',p;P) = \\ & \int \frac{d^4k'}{(2\pi)^4}\int \frac{d^4k}{(2\pi)^4}\left((2\pi)^4\delta^4(p'-k') - \mathcal{M}^\dagger(p',k';P)G_0^\dagger(k';P)\right) \\ & \times \left(V(k',k;P) - V^\dagger(k',k;P)\right) \\ & \times \left((2\pi)^4\delta^4(k-p) - G_0(k;P)\mathcal{M}(k,p;P)\right) \\ & - \int \frac{d^4k}{(2\pi)^4}\mathcal{M}^\dagger(p',k;P)\left(G_0(k;P) - G_0^\dagger(k;P)\right)\mathcal{M}(k,p;P). \end{aligned} \tag{7}$$

The discontinuity in the $\mathcal{M}$ matrix, which in this simple case is simply the imaginary part of the amplitude, arises from two contributions, one involving the discontinuity of the two-nucleon free propagator and the other involving the discontinuity of the kernel. The discontinuity of the free two-nucleon propagator is proportional to the product of two delta functions placing both of the nucleons on their mass shells. This can occur only when the $P^2 \geq (2m)^2$. If the invariant mass of the pair W is defined such that $P^2 = W^2$, then this can occur only when $W \geq 2m$ or $W \leq -2m$. Since the discontinuity of the free propagator occurs within a four-momentum loop, this produces branch cuts beginning at the two thresholds in W. These are the positive and negative energy elastic cuts. The discontinuity of the kernel is associated with

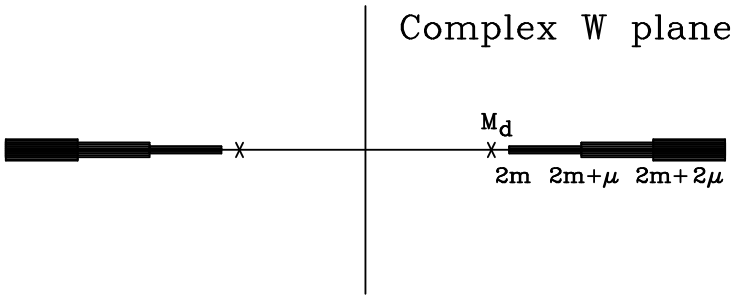

FIG. 4: The analytic structure of the $\mathcal{M}$ matrix as a function of complex W. The heavy lines represent branch cuts and crosses represent bound state poles.

both nucleons and at least one meson being on mass shell and contributes a set of overlapping cuts with thresholds at $W = \pm(2m + n\mu)$, where μ is the meson mass and $n > 0$ is an integer. The analytic structure of the $\mathcal{M}$ matrix as a function of complex W is shown in Fig. 4. Another possibility, that is obscured by writing the unitarity relation as in (7), is that the $\mathcal{M}$ matrix can have poles corresponding to the presence of bound states. For the purpose of discussion, assume that there is only one bound state for $P^2 = P_d^2 = M_d^2 < 4m^2$, where M_d is the mass of the scalar "deuteron." Thus, poles are expected in $\mathcal{M}$ at $W = \pm M_d$ and are illustrated in Fig. 4 by crosses.

The $\mathcal{M}$ matrix can now be represented as

$$\mathcal{M}(p', p, ; P) = \frac{\Gamma(p'; P_d)\Gamma^\dagger(p; P_d)}{P^2 - M_d^2 + i\eta} + \mathcal{R}(p', p, ; P), \tag{8}$$

where $\mathcal{R}(p', p, ; P)$ represents the remainder of the $\mathcal{M}$ matrix once the pole is removed. Substituting (8) into (1) gives

$$\begin{aligned}\frac{\Gamma(p'; P_d)\Gamma^\dagger(p; P_d)}{P^2 - M_d^2 + i\eta} + \mathcal{R}(p', p, ; P) &= V(p', p; P) \\ - \int \frac{d^4k}{(2\pi)^4} V(p', k; P) G_0(k; P) &\left(\frac{\Gamma(k; P_d)\Gamma^\dagger(p; P_d)}{P^2 - M_d^2 + i\eta} + \mathcal{R}(k, p, ; P) \right). \end{aligned} \tag{9}$$

Since V, G_0 and $\mathcal{R}$ are analytic at the bound state poles, comparing the residue of the pole on each side of the equation yields

$$\Gamma(p'; P_d) = - \int \frac{d^4k}{(2\pi)^4} V(p', k; P_d) G_0(k; P_d) \Gamma(k; P_d). \tag{10}$$

$\Gamma(p';P_d)$ is the Bethe-Salpeter bound state vertex function. The normalization of the bound state is obtained by first using (1) and (2) to obtain the nonlinear form of the Bethe-Salpeter equation

$$\mathcal{M}(p',p,;P) = V(p',p;P) - \int \frac{d^4k}{(2\pi)^4}\mathcal{M}(p',k;P)G_0(k;P)\mathcal{M}(k,p,;P) \\ - \int \frac{d^4k'}{(2\pi)^4}\int \frac{d^4k}{(2\pi)^4}\mathcal{M}(p',k';P)G_0(k';P)V(k',k;P)G_0(k;P)\mathcal{M}(k,p,;P). \tag{11}$$

Substituting (8) into (11) and equating the residues of the poles gives:

$$\begin{aligned} 1 &= \int \frac{d^4k}{(2\pi)^4}\Gamma^\dagger(k;P_d)\,\frac{\partial}{\partial P^2}G_0(k;P)\bigg|_{P_d}\Gamma(k;P_d) \\ &- \int \frac{d^4k'}{(2\pi)^4}\int \frac{d^4k}{(2\pi)^4}\Gamma^\dagger(k';P_d)G_0(k';P_d)\,\frac{\partial}{\partial P^2}V(k',k;P)\bigg|_{P_d}G_0(k;P_d)\Gamma(k;P_d), \end{aligned} \tag{12}$$

where the Bethe-Salpeter vertex equation (10) has been used to simplify the expression. The Bethe-Salpeter bound state wave function can now be defined as:

$$\psi(p;P_d) = G_0(p;P_d)\Gamma(p;P_d) \tag{13}$$

and, using the fact that $G_0(k';P_d)$ is hermitian, the wave function normalization is given by:

$$\begin{aligned} 1 &= \int \frac{d^4k}{(2\pi)^4}\psi^\dagger(k;P_d)G_0^{-1}(k;P_d)\,\frac{\partial}{\partial P^2}G_0(k;P)\bigg|_{P_d}G_0^{-1}(k;P_d)\psi(k;P_d) \\ &- \int \frac{d^4k'}{(2\pi)^4}\int \frac{d^4k}{(2\pi)^4}\psi^\dagger(k';P_d)\,\frac{\partial}{\partial P^2}V(k',k;P)\bigg|_{P_d}\psi(k;P_d) \end{aligned} \tag{14}$$

Using the definition of the wave function (13), and the equation for the vertex function (10) a wave equation can be written as

$$G_0^{-1}(p;P_d)\psi(p;P_d) = -\int \frac{d^4k}{(2\pi)^4}V(p,k;P_d)\psi(k;P_d) \tag{15}$$

The basic formalism is now in place for both scattering and normalized bound states. There are, however, substantial practical difficulties in obtaining such solutions. Although the equations as they are presented are exact, they can not be solved exactly since the kernel contains an infinite number of contributions. Therefore, it

is conventional to retain only a limited number of contributions to the kernel in order to obtain a solution. Typically, the kernel is truncated at the level of one- or two-boson exchange. This truncation constitutes an almost inevitable approximation and, as will be discussed below, for the scalar model used here, it is not the best approximation to the full untruncated Bethe-Salpeter equation.

A second problem, that is of a technical nature, is the difficulty of solving the four-dimensional integral equations. The equations can be reduced to two-dimensional equations by an expansion of the potentials, scattering matrices and vertex functions in some suitable set of angular functions. This leaves integrals in the loop energy and the magnitude of the loop momentum. As is usually the case with performing such loop integrations, it is convenient to perform a Wick rotation of the energy variable into the complex plane. Due to the presence of branch cuts associated with the angular expansion of the kernel, which move as a function of the external relative energy, the contour must be carefully distorted in performing the Wick rotation. The two-dimensional integral equations can, and have been solved numerically [4, 5, 6].

2.2 QUASIPOTENTIAL EQUATIONS

An alternate approach, to the construction of relativistic models of two-body bound and scattering states is the construction of quasipotential equations. This method can be understood in relation to the Bethe-Salpeter equations presented above. The common characteristic of all quasipotential equations is the replacement of the free two-nucleon propagator by a new propagator that includes a delta-function constraining the relative energy of the intermediate states and thereby reducing the four-dimensional integral equation to three dimensions. Although it is possible to express this replacement in completely covariant terms [26], it is most easily described in the center of momentum frame where the equations are generally actually solved. By introducing a new propagator of the form

$$g_0(p;P) = \frac{\pi}{E_p}\delta\left(p_0 - x(E_p - W/2)\right)\hat{g}_0(p;P), \tag{16}$$

where $E_p = \sqrt{\mathbf{p}^2 + m^2}$ is the on-mass-shell energy, the multiple scattering series represented by (1) can be rearranged into a pair of coupled integral equations

$$\mathcal{M}(p',p;P) = U(p',p;P) - \int \frac{d^3k}{(2\pi)^3 2E_k} U(p',\check{k};P)\hat{g}_0(\check{k};P)\mathcal{M}(\check{k},p;P), \tag{17}$$

and

$$U(p',p;P) = V(p',p;P) - \int \frac{d^4k}{(2\pi)^4} V(p',k;P)\left(G_0(k;P) - g_0(k;P)\right)U(k,p;P) \quad (18)$$

where $\check{k}$ represents the intermediate-state relative momentum constrained by the delta function in (16), and the new kernel in (17), defined by (18), is called the quasipotential. The equations (17) and (18) are exactly equivalent to (1). Note that while (17) is a three-dimensional integral equation, the equation for the quasipotential (18) is still four-dimensional. Matters have only been complicated at this stage by replacing one four-dimensional integral equation with a three-dimensional plus a four-dimensional integral equation. In practice, the (18) is not solved exactly, but is iterated and then truncated at a fixed number of meson exchanges. This reduces the construction of U to a quadrature over loops containing V. Indeed, in most cases, both the Bethe-Salpeter and quasipotential equations are solved in one-boson exchange or ladder approximation. In this approximation $U = V$.

The quasipotential equation for the vertex function is

$$\Gamma(p;P_d) = -\int \frac{d^3k}{(2\pi)^3 2E_k} U(p,\check{k};P_d)\hat{g}_0(\check{k};P_d)\Gamma(\check{k};P_d) \quad (19)$$

Note that the vertex function on the right side of (19) depends only upon the constrained relative momentum while the vertex function on the left depends upon the unconstrained momentum. The unconstrained vertex function is, therefore, obtained in two steps. First the integral equation is solved with only the constrained relative momentum $\check{p}$ appearing on the left of (19). The resulting constrained vertex function can then be substituted into the right side of (19) and the unconstrained vertex function obtained by quadrature. A similar approach can be applied to the solution of (17).

A constrained quasipotential wave function can be defined as

$$\hat{\psi}(\check{p};P_d) \equiv \hat{g}_0(\check{p};P_d)\Gamma(\check{p};P_d) \quad (20)$$

The normalization condition for these wave functions can be obtained in a similar fashion to that use in obtaining (14) and is

$$\begin{aligned} 1 &= \int \frac{d^3k}{(2\pi)^3 2E_k}\hat{\psi}^\dagger(\check{k};P_d)\hat{g}_0^{-1}(\check{k};P_d)\,\frac{\partial}{\partial P^2}\hat{g}_0(\check{k};P)\Big|_{P_d}\hat{g}_0^{-1}(\check{k};P_d)\hat{\psi}(\check{k};P_d) \\ &- \int \frac{d^3k'}{(2\pi)^3 2E_{k'}}\int \frac{d^3k}{(2\pi)^3 2E_k}\hat{\psi}^\dagger(\check{k}';P_d)\,\frac{\partial}{\partial P^2}U(\check{k}',\check{k};P)\Big|_{P_d}\hat{\psi}(\check{k};P_d) \end{aligned} \quad (21)$$

TABLE 1: A selection of quasipotential propagators for scalar nucleons

.

Name	x	$\hat{g}_0(\check{p}, P)$
Blankenbecler-Sugar [7]	0	$\frac{1}{2(E_p^2-\frac{W^2}{4})-i\eta}$
Thompson [8]	0	$\frac{1}{W(2E_p-W)-i\eta}$
Todorov [9]	0	$\frac{E_p}{W(E_p^2-\frac{W^2}{4})-i\eta}$
Gross (spectator) [12]	1	$\frac{1}{W(2E_p-W)-i\eta}$
Erkelenz-Holinde [10]	1	$\frac{1}{2(E_p^2-\frac{W^2}{4})-i\eta}$
Kadychevsky [11]	1	$\frac{1}{2E_p(2E_p-W)-i\eta}$
Gross [13]	$-1 \leq x \leq 1$	$\frac{2E_p}{W(2E_p-W)(E_p+\frac{W}{2}+x^2(E_p-\frac{W}{2}))}$

The wave equation for the constrained quasipotential wave function is

$$\hat{g}_0^{-1}(\check{p}; P_d)\hat{\psi}(\check{p}; P_d) = -\int \frac{d^3k}{(2\pi)^3 2E_k} U(\check{p}, \check{k}; P)\hat{\psi}(\check{k}; P_d) \tag{22}$$

Criteria for choosing $\hat{g}_0$ can be obtained by considering the analytic structure of the $\mathcal{M}$ matrix as shown in Fig. 4. Knowing the analytic structure, it is possible to construct dispersion relations for the scattering matrix. If the system is lightly bound, the physical values of W will be close to the elastic cut on the positive energy real W axis. The contributions to the scattering matrix coming from the positive energy cuts and poles should then constitute the dominant contributions to the scattering matrix. In order to preserve this property, it is necessary to choose $\hat{g}_0$ such that it preserves the position and residues associated with the positive energy elastic cut. This requirement allows for an infinite variety of choices for $\hat{g}_0$ and a substantial number of quasipotential propagators have been proposed in the literature. A representative sample for our scalar model is presented in Table 1.

Before examining the results of calculations performed in the simple scalar model,

it is useful to compare the Bethe-Salpeter and quasipotential equations. As a practical matter, both types of equations require that a truncated kernel be used for calculating scattering amplitudes and bound state wave functions, usually at the level of the ladder or one-boson-exchange approximation. The question then arises as to which of these equations provides the best approximation to the complete untruncated Bethe-Salpeter equation, which is the exact field-theoretical result. It is tempting to assume that the ladder approximation to the Bethe-Salpeter equation is the optimal approximation, in that it appears the most straightforward and least arbitrary prescription for truncating the equations. There is good reason to believe that this is not necessarily the case. The simple scalar model that is used here for pedagogical purposes has received a considerable amount of study. In particular, Gross [27] has examined this model in considerable detail and has shown that to all orders in the Feynman diagramatical expansion of the scattering matrix there is a partial cancellation between iterated ladder-like contributions and contributions from the crossed boxes. The particular organization of the $\mathcal{M}$ matrix equations associated with the spectator equation places the canceling pieces of the iterated ladders and the crossed boxes in higher-order contributions to the quasipotential and therefore improves the convergence of the truncated spectator equation to the full Bethe-Salpeter equation. This can also be seen in Table VI.1 of Ref. [26] which compares the coefficients of an expansion in μ/m of the second order contributions to the scattering matrix for several of the quasipotential equations and the full second order Bethe-Salpeter result. All of the approaches agree to order $(\mu/m)^{-1}$. All of the quasipotential approaches agree with the full second-order Bethe-Salpeter to order $(\mu/m)^0$, but the ladder approximation to the Bethe-Salpeter equation disagrees at this order. Some caution should be used in generalizing these results to systems involving particles with spin and isospin, in that the operators associated with these quantities can interfere with the delicate cancellations that occur in the scalar model. In these more complicated situations, the question of the quality of any particular approximation is still open. Some additional light can, however, be cast on the practical implications of this problem by some additional results from the study of the simple scalar model under conditions which approximate the use of these quasipotential equations in physical applications.

2.2.1 THIS IS A SUBSECTION

Four score and seven years ago, our forefathers brought forth on this continent a new nation conceived in liberty and dedicated to the proposition that all men are created equal.

2.3 THE SCALAR MODEL

It is useful to now construct a version of the scalar model that has features that appear in the calculations of the deuteron presented in Section VI. First, in any phenomenological model of the deuteron that treats the effective degrees of freedom as nucleons and mesons, information about the finite size of this constituents must be included as form factors at the interaction vertices. The general form of the nucleon-nucleon-meson vertex in our scalar model would be

$$-igF(p'^2, p^2, \ell^2) \tag{23}$$

where g is a dimensionful coupling constant, p and p' are the initial and final nucleon four-momenta, and $\ell = p - p'$ is the meson four-momentum. $F(p'^2, p^2, \ell^2)$ is a general form factor depending upon the invariant masses of the three virtual particles connecting to the interaction vertex. For simplicity, assume that the form factor can be written in a factorable form [14, 15, 28]

$$F(p'^2, p^2, \ell^2) = h(p'^2)h(p^2)f(\ell^2) \tag{24}$$

where the meson form factor is taken to be

$$f(\ell^2) = \frac{(\Lambda_\mu^2 - \mu^2)^2 + \Lambda_\mu^4}{(\Lambda_\mu^2 - \ell^2)^2 + \Lambda_\mu^4} \tag{25}$$

and the nucleon form factor is

$$h(p^2) = \frac{2(\Lambda_n^2 - m^2)^2}{(\Lambda_n^2 - p^2)^2 + (\Lambda_n^2 - m^2)^2} \tag{26}$$

where Λ_μ and Λ_n are meson and nucleon form factor masses. The presence of the nucleon form factor is an unusual feature of the calculations presented here. This form factor allows the four-momenta of the nucleons to be controlled such that the contributions from highly-virtual nucleons can be limited.

Since the model is to be solved for a variety of quasipotential equations, it is necessary to deal with an additional problem. For all quasipotential propagators for which $x \neq 0$, the intermediate state nucleons in (17) are not treated symmetrically.

This can lead to problems with the Pauli exchange symmetry of the scattering amplitudes and vertex functions. It has been shown in Ref. [15] that this problem can be overcome by requiring that the interaction kernel be symmetrized for bosons or antisymmetrized for fermions. Therefore, the kernel for the quasipotential equations should be taken as

$$\begin{aligned} V(p',p;P) &= \frac{1}{2}g^2 h((P/2+p')^2)h((P/2-p')^2) \\ &\quad \times \left[f((p-p')^2)\Delta_F(p-p',\mu) + f((p+p')^2)\Delta_F(p+p',\mu)\right] \\ &\quad \times h((P/2+p)^2)h((P/2-p)^2). \end{aligned} \tag{27}$$

for the scalar model, where it is assumed that the exchanged meson carries no charge. This procedure has the drawback that it can generate spurious singularities in the calculation of scattering amplitudes and vertex functions. This problem can be dealt with as shown in Ref. [15].

It is useful to use a procedure in choosing the parameters in the model that is consistent with the methods used to constrain the model parameters in meson-nucleon models of the deuteron. Any acceptable model of the deuteron must contain an interaction that produces the deuteron bound state at the correct binding energy and that provides a reasonable description of the scattering data up to a few hundred MeV of laboratory kinetic energy. Since it is intended that this scalar model bear some resemblance to the deuteron, the scalar nucleon mass is chosen to be $m = 938.9\ MeV$, the meson mass to be $\mu = 138.0\ MeV$ and the meson form factor mass is fixed to be $\Lambda_\mu = 2500.0\ MeV$, which is of the same order as the meson form factor masses found in the fits to the deuteron and the NN scattering data in Refs. [14, 15]. For each calculation, the value of the nucleon form factor mass is fixed, but various values of this parameter are considered in order to examine the sensitivity of the calculations to this parameter. If the nucleon, meson and form factor masses are fixed, the only remaining parameter in this simple scalar model is the coupling constant. The procedure used in producing these calculations for the scalar model is to adjust the coupling constant for each quasipotential model to produce an S-wave bound state at a binding energy of 2.3 MeV. This value is then used to calculate the S- and D-wave phase shifts for the model.

Figure 5 shows the values of the square of the coupling constants for the various quasipotential models listed in Table I as a function of the quasipotential parameter x. The crosses are calculated with a nucleon form factor mass $\Lambda_n = 1600\ MeV$,

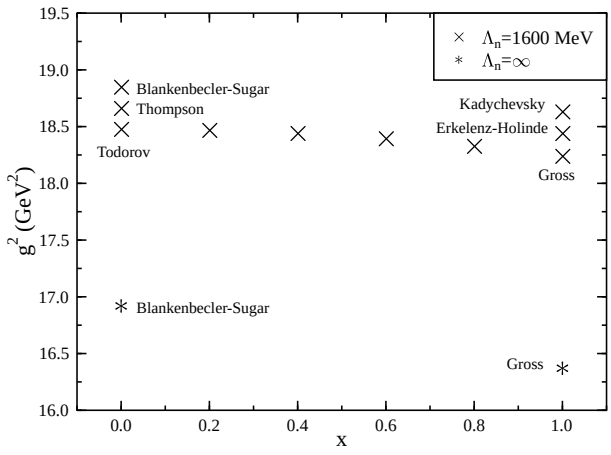

FIG. 5: This figure shows square of the coupling constants for the various quasipotential models listed in Table I. The crosses represent couplings calculated with a nucloen form factor mass of $\Lambda_n = 1600\ MeV$. The asterisks represent couplings calculated with $\Lambda_n = \infty$.

and the asterisks are calculated with $\Lambda_n = \infty$. Values for $-1 < x < 1$ are for the family of quasipotential models described in Ref. [13]. Clearly, the coupling constant depends both on the quasipotential model used and the value of the nucleon cutoff. However, for a fixed cutoff mass, the variation in the value of g^2 is on the order of a few percent. In these models, the couplings should be viewed as effective coupling constants.

Figure 6 shows S- and D-wave phase shifts calculated for the various quasipotential models with $\Lambda_n = 1600\ MeV$. The phase shifts for all models are within 0.5 degrees over the range $0 < T_{lab} < 300\ MeV$. This implies that there is very little model dependence once the coupling constants are fixed to give the same binding energy. This is in contrast with the results shown in Fig. 17 of Ref. [26] where the coupling constant was fixed arbitrarily and considerable variation was seen in the phase shifts. Figure 7 shows a comparison of the range of phase shifts calculated with $\Lambda_n = 1600\ MeV$ (light shading) with those with $\Lambda_n = \infty$ (small cross-hatched band). The spread in values of the phase shifts with $\Lambda_n = \infty$ is still small, however, a substantial sensitivity to the cutoff mass is apparent. If phase shift data were available for this model and included in the fit, as is the case with the NN interaction

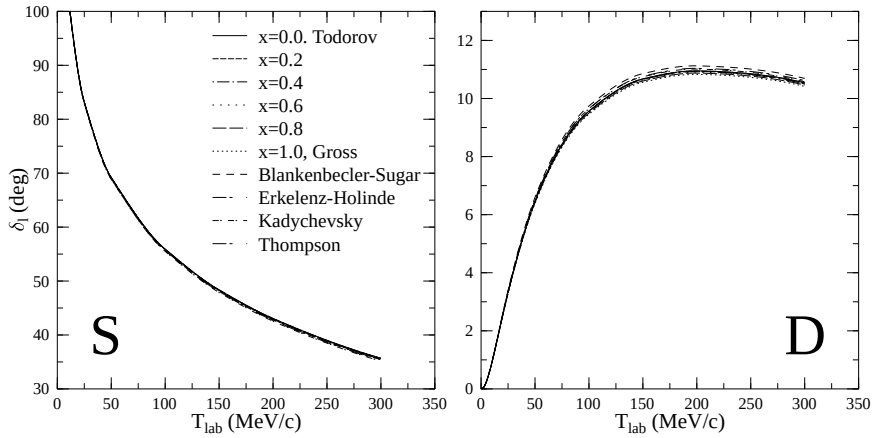

FIG. 6: S- and D- wave phase shifts calculated for the various models listed in Table I with $\Lambda_n = 1600\ MeV$.

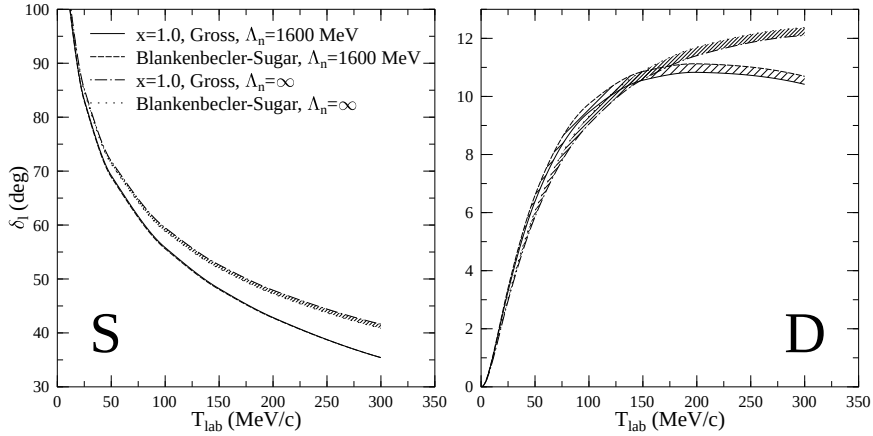

FIG. 7: S- and D- wave phase shifts calculated for the various models listed in Table I comparing results with $\Lambda_n = 1600\ MeV$ (light shading) to those with $\Lambda_n = \infty$ (dark shading).

models, the fit would tend to constrain the value of any parameter which tended to generate substantial variation in the phase shifts.

Figure 8 shows the constrained quasipotential momentum-space wave functions calculated for the various models listed in Table 1. All of the wave functions give similar values below about 200 MeV but tend to diverge as the momentum increases. This is not an unexpected result since the quasipotential propagators are very similar at low p but will differ increasingly from one another as the momentum increases. Similarly, the effect of the nucleon cutoff will become more apparent at larger momenta.

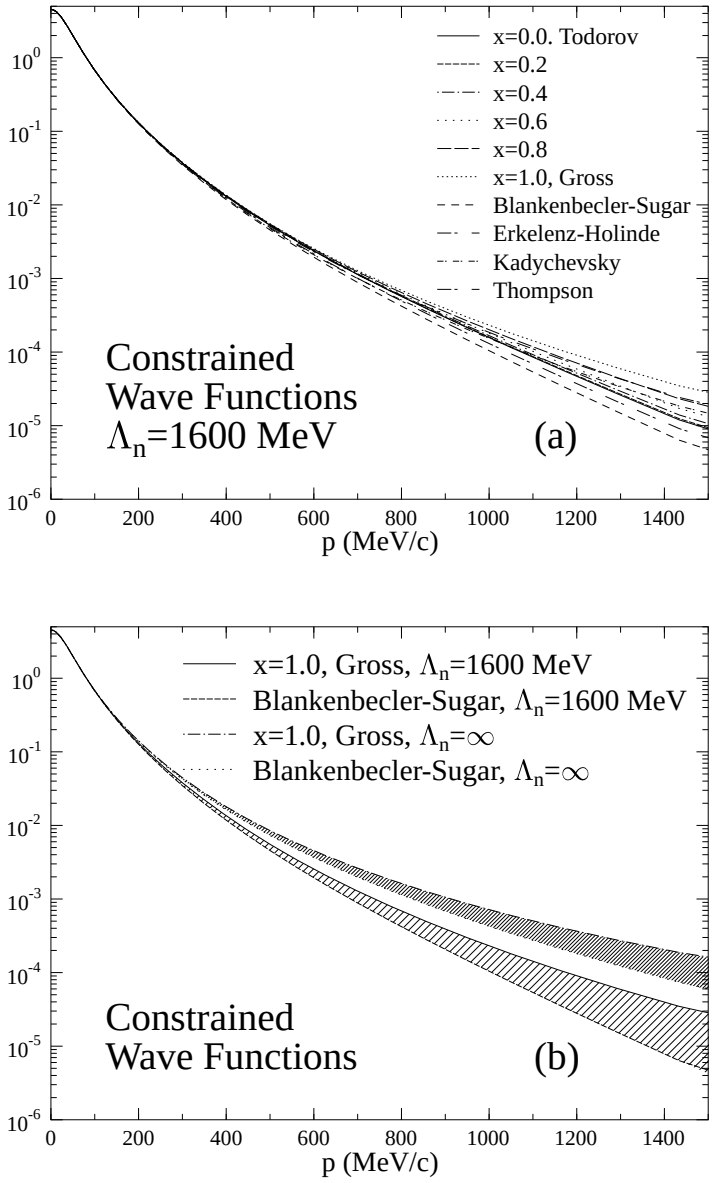

FIG. 8: Constrained quasipotential momentum space wave functions calculated for the various models listed in Table I. Figure (a) shows the various models with $\Lambda_n = 1600\ MeV$, while the Fig. (b) compares this range of results with that with $\Lambda_n = \infty$.

CHAPTER 3

ELECTROMAGNETIC INTERACTIONS

3.1 ELECTROMAGNETIC CURRENT FOR THE BETHE-SALPETER EQUATION

In order to describe the electromagnetic properties of the deuteron, it is necessary to be able to construct the electromagnetic current matrix elements for the interacting two-nucleon system. To see how this is done, consider the Feynman diagrams describing two-nucleon scattering in Fig. 1. If it is assumed that both the nucleons and the mesons can carry charge, then it is expected that an external electromagnetic field should see currents associated with the motion of both nucleons and mesons. The five-point function describing the interaction of a virtual photon with the scattering nucleons can then be represented by all Feynman diagrams which can be obtained by attaching the virtual photon to each of the nucleon and meson lines in Fig. 1. The diagrams can then be used to identify single-nucleon currents and two-nucleon irreducible two-body currents. The matrix element associated with elastic electron scattering from the Bethe-Salpeter two-nucleon bound state can then be represented by the the Feynman diagrams in Fig. 9. The two-nucleon irreducible electromagnetic interaction current is represented by the diagrams in Fig. 10. These two-nucleon currents are usually referred to as meson exchange currents (MEC).

In the simple scalar model, the Feynman rules can be used to represent the three diagrams in Fig. 9 as

$$\begin{aligned}
\mathcal{J}^{\mu}(P',P) &= -\int \frac{d^4p'}{(2\pi^4)} \int \frac{d^4p}{(2\pi^4)} \psi^{\dagger}(p';P') \\
&\times \left\{ iJ^{(1)\mu}\left(\frac{P'}{2}+p',\frac{P}{2}+p\right) \Delta_F^{(2)^{-1}}\left(\frac{P'}{2}-p',m\right) \right. \\
&\quad \times (2\pi)^4\delta^4\left(\frac{P'}{2}-p'-\frac{P}{2}+p\right) \\
&\quad + iJ^{(2)\mu}\left(\frac{P'}{2}-p',\frac{P}{2}-p\right) \Delta_F^{(1)^{-1}}\left(\frac{P'}{2}+p',m\right) \\
&\quad \left. \times (2\pi)^4\delta^4\left(\frac{P'}{2}+p'-\frac{P}{2}-p\right) + J^{(12)\mu}(p',P';p,P) \right\} \psi(p;P) \quad (28)
\end{aligned}$$

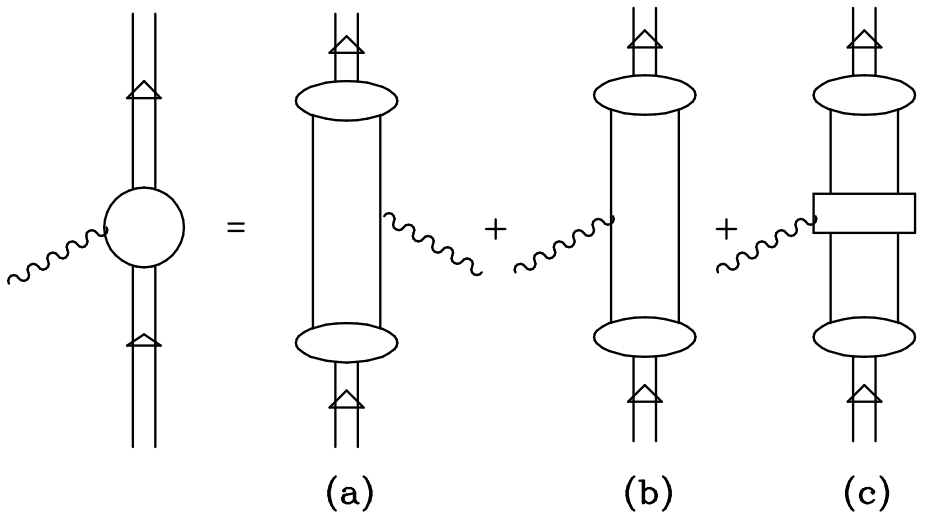

FIG. 9: Feynman diagrams representing the Bethe-Salpeter matrix element for elastic electron scattering form the two-nucleon bound state

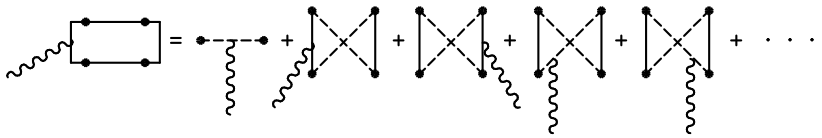

FIG. 10: Feynman diagrams representing the two-nucleon irreducible electromagnetic interaction current.

where $J^{(i)\mu}(p'_i, p_i)$ is the single-nucleon current operator for nucleon i and $J^{(12)\mu}(p', P'; p, P)$ is the two-nucleon irreducible current operator.

The single-nucleon current must satisfy the Ward-Takahashi identity [29]

$$q_\mu J^{(i)\mu}(p', p) = \Delta_F^{-1}(p', m) - \Delta_F^{-1}(p, m). \tag{29}$$

Contracting the current matrix element (28) with q_μ and using the wave equation (15), it can be shown that the two-nucleon current operator must satisfy the identity [28]

$$\begin{aligned} q_\mu J^{(12)\mu}(p', P'; p, P) &= V(p' + \frac{q}{2}, p; P) + V(p' - \frac{q}{2}, p; P) \\ &\quad - V(p', p + \frac{q}{2}; P') - V(p', p - \frac{q}{2}; P') \end{aligned} \tag{30}$$

If the model calculations were strictly field theoretical, there would now be no additional complications, since the usual field theoretical couplings to the nucleon and meson for the diagrams of Fig. 10 would satisfy (30) provided that the kernel and the two-nucleon current were truncated at the same number of meson exchanges. The complication comes from the introduction of form factors at the strong and electromagnetic vertices to account for the finite sizes of the nucleons and mesons. For example, it is tempting to simply write the phenomenological electromagnetic one-body current for the nucleon as the field theoretical bare coupling multiplied by a form factor to give

$$J^{(i)\mu}(p', p) = F(Q^2)(p' + p)^\mu \tag{31}$$

where $Q^2 = -q^2 = -(p' - p)^2$. This does not satisfy the Ward-Takahashi identity, however. This problem has been studied in Ref. [28] for models containing factorable vertices such as is defined by (23) and (24). It is shown there that this problem can be dealt with if the electromagnetic current is taken to be

$$J^{(i)\mu}(p', p) = a(Q^2, p'^2, p^2) \left[(p' + p)^\mu - \frac{(p' + p) \cdot q}{q^2} q^\mu \right] + b(p'^2, p^2)(p' + p)^\mu \tag{32}$$

where

$$b(p'^2, p^2) = f_0(p'^2, p^2) = \left[\frac{h(p^2)}{h(p'^2)}(p'^2 - m^2) - \frac{h(p'^2)}{h(p^2)}(p^2 - m^2) \right] \frac{1}{p'^2 - p^2} \tag{33}$$

and

$$a(Q^2, p'^2, p^2) = (F(Q^2) - 1) h_0(Q^2, p'^2, p^2) \tag{34}$$

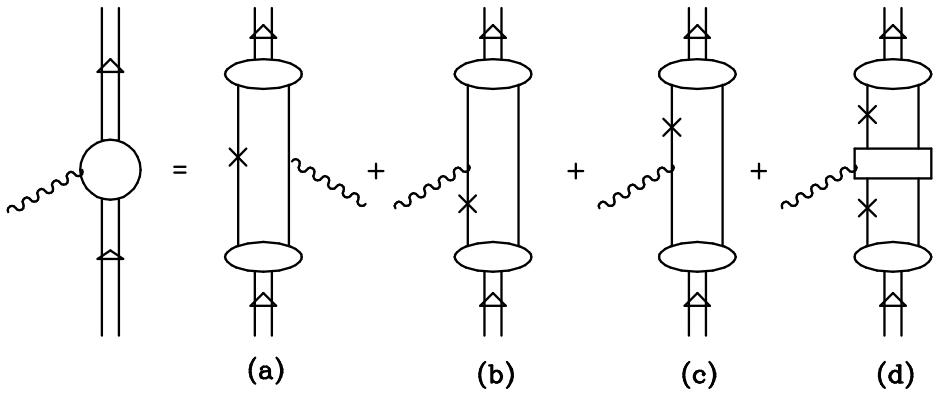

FIG. 11: Feynman diagrams representing the elastic current matrix element for the spectator or Gross equation

where h_0 is some function subject to the constraint $h_0(Q^2, m^2, m^2) = 1$. The choice $h_0(Q^2, p'^2, p^2) = f_0(p'^2, p^2)$ is used here for simplicity. A similar procedure must be followed in general for the electromagnetic current of the meson. For the calculations presented here, a single-nucleon form factor of the form

$$F(Q^2) = \frac{1}{\left(1 + \frac{Q^2}{0.71 GeV^2}\right)^2} \tag{35}$$

is used.

3.2 ELECTROMAGNETIC CURRENT FOR THE SPECTATOR EQUATION

Construction of the correct form of the current matrix element for the truncated quasipotential has not been sufficiently studied for the general case. However, the correct form of the matrix element for the spectator or Gross equation has been described in Ref. [28], and a description of the matrix element for the Blankenbecler-Sugar equation is described in a recent paper by Coester and Riska [25]. The spectator equation will be used for the calculations of the electromagnetic current presented here for the scalar model and for the realistic deuteron calculation.

The motivation for the construction of the current matrix element for the spectator equation can be most easily seen by realizing that the choice of the spectator equation propagator is equivalent to keeping only the positive energy nucleon pole for

particle 1 in all loop integrations. Now, consider the diagrams for the Bethe-Salpeter current matrix element in Fig. 9. For diagram (9a), particle 1 can be placed on its positive energy mass shell leading to diagram (11a), where the on-shell particle is represented by a cross. In the case of Fig. 9b, particle 1 can be placed on mass shell either before or after the interaction with the virtual photon leading to the two diagrams (11b) and (11c). Diagram (9c) contains two loops and particle 1 can be placed on shell in both of them leading to diagram (11c). In this last case, the two-nucleon current will be the same as the Bethe-Salpeter two-nucleon current only at the level of one meson exchange. Note that while diagrams (11a) and (11d) require only the constrained vertex functions, diagrams (11b) and (11c) require both the constrained and the unconstrained vertex functions.

Prior to Ref. [28], it was assumed that the proper form of the current matrix element was described by diagram (11a) along with a symmetric diagram where the photon attaches to particle 1 and particle 2 is placed on mass shell [17]. Because of the symmetry of the matrix element, the contribution of the second diagram is equivalent to diagram (11a). Thus this approximation is equivalent to simply calculating 2×diagram (11a). Since the form of this approximation looks like a matrix element of a single-nucleon current between spectator wave functions, it is referred to as the relativistic impulse approximation (RIA). However, it has been shown that the RIA does not, in general, conserve the electromagnetic current while the complete matrix element, described by the diagrams of Fig. 11, does [28].

For elastic scattering from the scalar deuteron, Lorentz invariance and current conservation require that the current matrix element be of the form

$$\mathcal{J}^{\mu}(P',P) = G(Q^2)(P'^{\mu} + P^{\mu}) \tag{36}$$

where $G(Q^2)$ is the elastic form factor with $Q^2 = -(P'-P)^2$. The form factor is defined such that $G(0) = 1$, since at long wave lengths only the total charge of the scalar deuteron can be measured. The symptom of the lack of current conservation in the RIA is manifest as $G_{RIA}(0) \neq 1$.

Figure 12 shows the square of the form factor of the scalar deuteron calculated using the spectator equation. Fig. 12a shows three calculations of the RIA, one with $f_0 = 1$ for $\Lambda_n = 1600\ MeV$, one with the single-nucleon current as given in (32) (labeled as $f_0 \neq 1$) for $\Lambda_n = 1600\ MeV$, and a the third is calculated with $\Lambda_n = \infty$. Note that the use of the off-shell current operator (32) results in a substantial increase

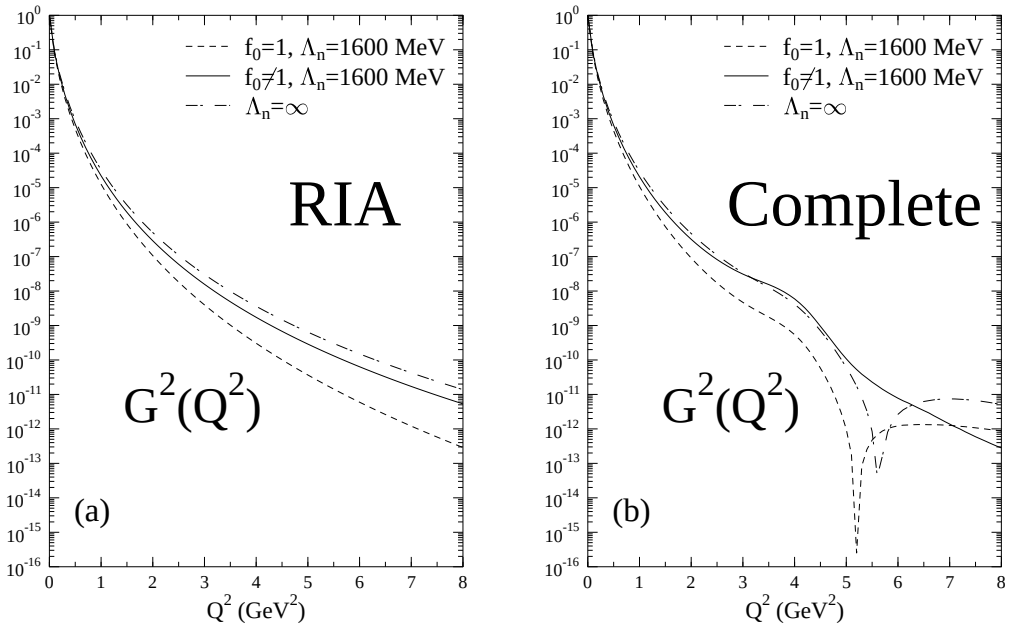

FIG. 12: The square of the electric form factor of the scalar deuteron. Figure (a) shows three calculations in the RIA while figure (b) shows similar calculations for the complete current conserving matrix element.

in the size of the form factor at large momentum transfers, bringing it much closer to the result with no nucleon cutoff. Figure 12b shows the complete calculation resulting from the sum of diagrams (11a), (11b) and (11c), where, in this case, diagram (11d) does not contribute since it is assumed that the meson carries no charge. Three calculations are presented which correspond to those of Fig. 12a. The basic trends are as in the RIA. However, it is clear that calculation of the complete conserved current can result in a substantial modification of the form factor at larger momentum transfers from that obtained in the RIA.

CHAPTER 4

MODEL OF THE PHYSICAL DEUTERON

All of the basic conceptual machinery is now in place to extend the simple scalar model calculations to the more realistic case of spin-$\frac{1}{2}$, isospin-$\frac{1}{2}$ nucleons interacting through the exchange of a variety of mesons with various masses, spins, parities and isospins. All quantities can be calculated just as in the scalar case, but the calculations are complicated considerably by the necessity of dealing with relativistic particles with spin. The spin-$\frac{1}{2}$ nucleons are now defined by propagators which are four-dimensional matrices in the Dirac-spinor space and couplings of mesons to the nucleons are in general represented by operators in the Dirac-space and operators in the isospin space of the nucleons. Therefore, many of the quantities which are simply represented by numbers in the scalar model will be matrices or tensors in the realistic model. While tedious, these complications can be dealt with in relatively straight forward ways by constructing coupled integral equations projected onto suitable subspaces. It is useful to examine some of the quantities which contribute to the realistic calculation in order to understand how to extend the previous discussion to cover the more realistic model.

The Bethe-Salpeter vertex function for the spin-1 deuteron can be written as

$$\left(\Gamma(p,P)\cdot\xi_{\lambda_d}(P)\mathcal{C}\right)_{ab} \tag{37}$$

where $\xi_{\lambda_d}(P)$ is the polarization four-vector for the deuteron, $\mathcal{C}$ is the Dirac charge conjugation matrix , the subscripts a and b are indices in the Dirac spinor space, and Γ^μ can be determined by basic symmetry arguments to have the general form:

$$\begin{aligned}
\Gamma^\mu(p,P) \;=\;& f_1(p^2,p\cdot P)\gamma^\mu + g_1(p^2,p\cdot P)\frac{p^\mu}{m} \\
&+\frac{\not{p}_2 - m}{m}\left(f_2(p^2,p\cdot P)\gamma^\mu + g_2(p^2,p\cdot P)\frac{p^\mu}{m}\right) \\
&+\left(f_2(p^2,-p\cdot P)\gamma^\mu + g_2(p^2,-p\cdot P)\frac{p^\mu}{m}\right)\frac{\not{p}_1 + m}{m} \\
&+\frac{\not{p}_2 - m}{m}\left(f_4(p^2,p\cdot P)\gamma^\mu + g_4(p^2,p\cdot P)\frac{p^\mu}{m}\right)\frac{\not{p}_1 + m}{m}
\end{aligned} \tag{38}$$

where $p_1 = \frac{P}{2} + p$ and $p_2 = \frac{P}{2} - p$. This satisfies the generalized Pauli symmetry requiring that

$$\Gamma^{\mu}(p,P) = -\mathcal{C}\Gamma^{\mu T}(-p,P)\mathcal{C}^{-1}. \tag{39}$$

Note that for given values of p and P, the vertex function depends upon eight scalar functions, two pairs of which are related by inversion of p. In the case of the constrained spectator vertex function where particle 1 is on its positive energy mass shell, only four of these functions contribute. Therefore, the general Bethe-Salpeter vertex and wave functions can be represented by eight radial wave functions while the spectator constrained vertices and wave functions have only four radial wave functions.

The single-nucleon current operator to be used with factorable interaction vertices is given by [28]:

$$\begin{aligned} J^{(i)\mu}(p',p) &= F_1(Q^2) f_0(p'^2,p^2)\,\gamma^{\mu} + \frac{F_2(Q^2)}{2m} h_0(p'^2,p^2)\, i\sigma^{\mu\nu}q_{\nu} \\ &\quad + F_3(Q^2) g_0(p'^2,p^2)\,\frac{\not{p}' - m}{2m}\,\gamma^{\mu}\,\frac{\not{p} - m}{2m} \end{aligned} \tag{40}$$

where

$$f_0(p'^2,p^2) \equiv \frac{h(p^2)}{h(p'^2)}\,\frac{m^2 - p'^2}{p^2 - p'^2} + \frac{h(p'^2)}{h(p^2)}\,\frac{m^2 - p^2}{p'^2 - p^2}, \tag{41}$$

$$g_0(p'^2,p^2) \equiv \left(\frac{h(p^2)}{h(p'^2)} - \frac{h(p'^2)}{h(p^2)}\right)\frac{4m^2}{p'^2 - p^2} \tag{42}$$

and $h_0(p'^2,p^2)$ is an arbitrary function subject only to the constraint that $h_0(m^2,m^2) = 1$. In the calculations presented here, this function is chosen to be $h_0(p'^2,p^2) = f_0(p'^2,p^2)$, for simplicity.

By invoking Lorentz invariance, current conservation and parity, the general form of the elastic electromagnetic current matrix element for elastic electron scattering from the deuteron can be shown to have the general form [17]:

$$\begin{aligned} \mathcal{J}^{\mu}_{\lambda'_d\lambda_d}(P',P) &= -\Big\{ G_1(Q^2)(\xi^*_{\lambda'_d}(P')\cdot\xi_{\lambda_d}(P))(P'+P)^{\mu} \\ &+ G_2(Q^2)\Big[\xi^{\mu}_{\lambda_d}(P)(\xi^*_{\lambda'_d}(P')\cdot q) - \xi^{\mu *}_{\lambda'_d}(P')(\xi_{\lambda_d}(P)\cdot q)\Big] \\ &- G_3(Q^2)\frac{1}{2M_d^2}(\xi^*_{\lambda'_d}(P')\cdot q)(\xi_{\lambda_d}(P)\cdot q)(P'+P)^{\mu}\Big\} \end{aligned} \tag{43}$$

The G_i's are related to the charge, magnetic and quadrupole form factors by:

$$\begin{aligned} G_C &= G_1 + \frac{2}{3}\eta G_Q \\ G_M &= G_2 \\ G_Q &= G_1 - G_2 + (1+\eta)G_3 \end{aligned} \tag{44}$$

TABLE 2: This is a spurious table.

	U	T_{10}	T_{20}	$Im\ T_{11}$	ReT_{11}	ImT_{21}	ReT_{21}	ImT_{22}	ReT_{22}
U	I	I	I	II	II	II	II	I	I
P_n	I	I	I	II	II	II	II	I	I
P_s	II	II	II	I	I	I	I	II	II
P_l	II	II	II	I	I	I	I	II	II

where

$$\eta = \frac{Q^2}{4M_d^2} \tag{45}$$

The cross section for elastic electron-deuteron scattering is:

$$\frac{d\sigma}{d\Omega} = \left(\frac{d\sigma}{d\Omega}\right)_{Mott} \frac{1}{1+\frac{2E}{M_d}\sin^2(\theta/2)} \left[A(Q^2) + B(Q^2)\tan^2\frac{\theta}{2}\right] \tag{46}$$

where the structure functions $A(Q^2)$ and $B(Q^2)$ can be defined in terms of the form factors G_C, G_M and G_Q as:

$$\begin{aligned} A(Q^2) &\equiv G_C^2(Q^2) + \frac{Q^2}{6M_d^2}G_M^2(Q^2) + \frac{Q^4}{18M_d^4}G_Q^2(Q^2) \\ B(Q^2) &\equiv \frac{Q^2}{3M_d^2}\left(1+\frac{Q^2}{4M_d^2}\right)G_M^2(Q^2) \end{aligned}$$

The charge and quadrupole form factors can be separated by measuring the tensor polarization T_{20} in a polarization experiment. This is defined as:

$$T_{20}(Q^2) = -\frac{\sqrt{2}Q^2}{3M_d^2}\frac{G_C G_Q + (Q^2/12M_d^2)G_Q^2}{G_C^2 + (Q^4/18M_d^4)G_Q^2} \tag{47}$$

and is sometimes denoted as $\tilde{t}_{20}$.

Reference [15] describes in considerable detail the application of the spectator equation to nucleon-nucleon scattering and the deuteron bound state. Four models are presented for the NN interaction. Each model has been fitted to the NN phase shift data of Arndt and Roper, SP89 [30] with the aid of the error matrix obtained in the phase shift fit. These fits are constrained such that the deuteron bound state mass is correct. The resulting phase shift calculations are then compared to the data base and typically obtain a χ^2 per datum of approximately 2 for energies from 0 MeV to

225 MeV of laboratory kinetic energy. This is quite good for a one-boson-exchange model.

An unusual feature of these calculations is that some care has been taken in allowing for meson-nucleon couplings that contain off-shell couplings which are not usually present in such models. For example, the basic form of the πNN coupling is chosen to be [14, 15, 16]:

$$g_\pi \left[\lambda_\pi \gamma^5 + (1 - \lambda_\pi) \frac{(\not{p} - \not{p}')}{2m} \gamma^5 \right] \tag{48}$$

where $0 \leq \lambda_\pi \leq 1$ is a parameter which extrapolates the coupling between pseudoscalar and pseudovector coupling. This coupling is independent of λ_π when the nucleons are on mass shell, so models with differing values of λ_π differ in their off-shell content. All meson-nucleon interactions also include factorable form factors as in the scalar model presented above.

Two of the models from Refs. [14, 15] are used in the calculations of elastic electron-deuteron scattering that will be presented here. These models are labelled Model IB and Model IIB. Model IB has a kernel containing four mesons: π, σ, ω and ρ. The pion mixing parameter λ_π was adjusted as part of the fitting procedure and has a value of $\lambda_\pi = 0.216$. That is, there is a 22% admixture of pseudo-scalar pion coupling. A total of ten parameters are adjusted in the fitting procedure. Model IIB has six mesons: π, η, σ, σ_1, ω and ρ. The σ_1 meson is a scalar-isovector companion to the σ with a mass comparable to the σ mass. The pion mixing parameter was fixed at $\lambda_\pi = 0$ for pure pseudovector coupling. A total of thirteen parameters were adjusted in the fitting procedure.

Figure 13 shows preliminary results for the A and B structure functions as calculated for models IB and IIB using the Galster form of the dipole parameterization of the single-nucleon electromagnetic form factors [31]. Four calculations are presented for each case. The full calculation is the result of calculating diagrams (11a), (11b) and (11c). Since the deuteron is an isoscalar, the only exchange currents as represented by diagram (11d) must be isoscalar and in this case are transition currents of the type $\rho\pi\gamma$. Such corrections are in the process of being calculated for these models, but are not yet available. The three remaining calculations are RIA calculations. One uses the usual on-shell current operator which corresponds to setting $f_0 = h_0 = 1$ and g_0 and is labelled "RIA". The second uses the full off-shell current described by (40) and is labelled "RIA, off shell". The third is the Bethe-Salpeter

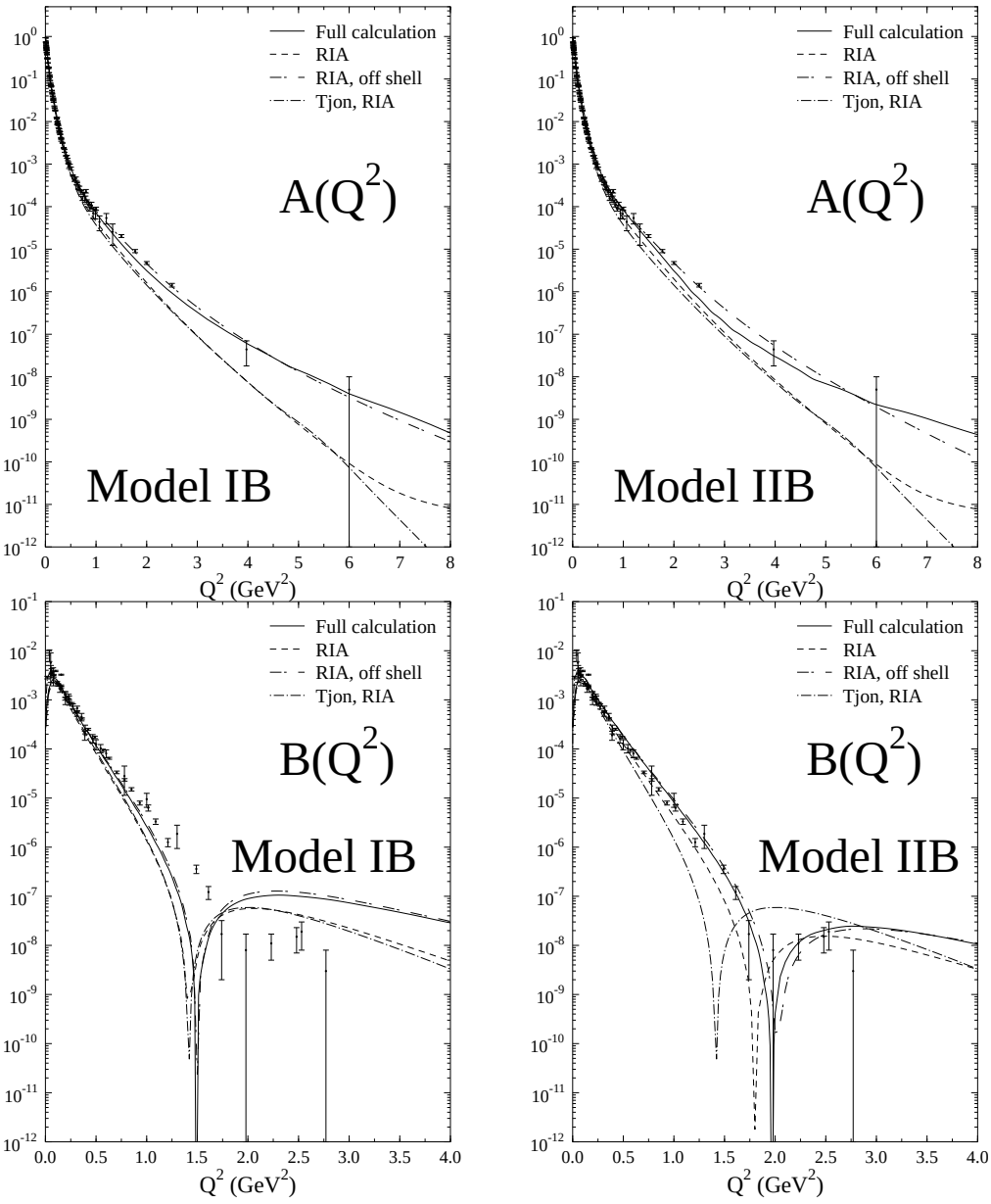

FIG. 13: A and B structure functions for models IB and IIB using the spectator equation.

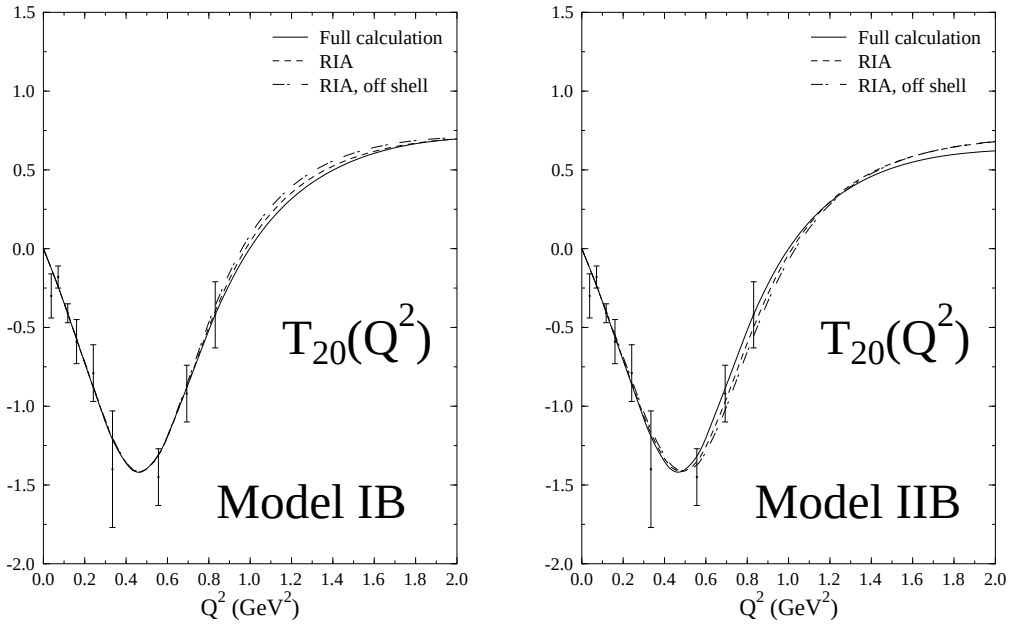

FIG. 14: T_{20} for models IB and IIB using the spectator equation.

RIA of Zuilhof and Tjon [5] which corresponds to diagrams (9a) and (9b), only the usual form of the on-shell current operator is used. Use of the off-shell single-nucleon current causes an increase in size for all of the structure functions. The full calculations show little model dependence for $A(Q^2)$. The full calculations of $A(Q^2)$ are still somewhat below the data at intermediate Q^2 and will require some contribution from isoscalar exchange currents, although less than previous calculations. $B(Q^2)$ shows substantial model dependence with the position of the diffraction minimum moved to higher Q^2. Indeed, the full calculation is in remarkably good agreement with the data. This calculation may indeed be too good in that it leaves little room for exchange current contributions. There is, however, some controversy as to the strength of the isoscalar exchange currents with recent calculations suggesting that they may, indeed, be small [32]. Since models IB and IIB are largely equivalent on mass shell, the sensitivity of $B(Q^2)$ is likely the result of the off-mass-shell differences of the two interactions. This suggests that electromagnetic processes may well provide useful information about the off-shell behavior of strong interaction models.

Figure 14 shows $T_{20}(Q^2)$ for models IB and IIB. This function shows little sensitivity to the various approximations or to the difference in models. All calculations

are in reasonable agreement with the data.

CHAPTER 5

CONCLUSIONS

This paper provides an introduction to the Bethe-Salpeter and related quasipotential equations. A simple scalar model is introduced to show the features of the solutions of these equations. This model shows that, provided the coupling is adjusted to reproduce the bound-state mass, the phase shifts display little variation among a representative collection of quasipotential equations. This feature needs to be studied in more detail for more complicated and realistic models. Care must be taken in constructing the electromagnetic current matrix elements for these covariant equation in order that gauge invariance not be violated.

Preliminary calculations are presented for the elastic structure functions of the deuteron using realistic meson-nucleon models. These models provide a reasonable description of the structure functions. In particular the calculation of $B(Q^2)$ using model IIB is the best representation of this structure function yet obtained in the context of such covariant models.

Considerable work remains to be done in extending these calculations to other reactions and in the study of the relative characteristics of the various relativistic approaches.

BIBLIOGRAPHY

[1] B. D. Keister and W. N. Polyzou, Adv. Nucl. Phys. **20**, 225 (1961).

[2] P. L. Chung, F. Coester, B. D. Keister, and W. N. Polyzou, Phys. Rev. C **37**, 2000 (1988).

[3] E. E. Salpeter and H. A. Bethe, Phys. Rev. **84**, 1232 (1951).

[4] J. Fleischer and J. A. Tjon, Nucl. Phys. **B84**, 375 (1975); Phys. Rev. D **15**, 2537 (1977); **21**, 87 (1980). E. van Faassen and J. A. Tjon, Phys. Rev. C **28**,2354 (1983); **30**, 285 (1984); **33**, 2105 (1986).

[5] M. J. Zuilhof and J. A. Tjon, Phys. Rev. C **22**, 2369 (1980); **24**, 736 (1981).

[6] A. Yu. Umnikov and F. C. Khanna, Phys. Rev. C **49** 2311 (1994).

[7] R. Blankenbecler and R. Sugar, Phys. Rev. **142**, 1051 (1966); A. A. Logunov and A. N. Tavkhelidze, Nuovo Cimento **29**, 380 (1963).

[8] R. H. Thompson, Phys. Rev. D **1**, 1738 (1970).

[9] I. T. Todorov, Phys. Rev. D **10**, 2351 (1971).

[10] K. Erkelenz and K. Holide, Nucl. Phys. **A194**, 161 (1972).

[11] V. G. Kadychevsky, Nucl. Phys. **B6**, 125 (1968).

[12] F. Gross, Phys. Rev. **186**, 1448 (1969); Phys. Rev. D **10**, 223 (1974).

[13] F. Gross,Phys. Rev. C **26**, 2203 (1982).

[14] F. Gross, J. W. Van Orden and K. Holinde, Phys. Rev. C **41**, R1909 (1990).

[15] F. Gross, J. W. Van Orden and K. Holinde, Phys. Rev. C **45**, 2094 (1992).

[16] W. W. Buck and F. Gross, Phys. Rev. D **20**, 2361

[17] R. E. Arnold, C. E. Carlson, and F. Gross, Phys. Rev. C **21**, 2361 (1980).

[18] E. Hummel and J. A. Tjon, Phys. Rev. Lett. **63**, 1788 (1989).

[19] S. J. Wallace and V. B. Mandelzweig, Nucl. Phys. **A503**, 673 (1989).

[20] N. K. Devine and S. J. Wallace, Phys. Rev. C **48**, 973 (1993).

[21] X. Zhu, R. Gourishankar, F. C. Khanna, G. Y. Leung, and N. Mobed, Phys. Rev. C **45**, 959 (1992).

[22] M. G. Fuda, Phys. Rev. D **44**, 1880 (1991).

[23] V. A. Karmanov and A. V. Smirnov, Nucl. Phys. **A546**, 691 (1992).

[24] D. Lurie, *Particles and Fields*, (Wiley-Interscience, London, 1968).

[25] F. Coester and D. O. Riska, Preprint nucl-th 9309026.

[26] G. E. Brown and A. D. Jackson, *The Nucleon–Nucleon Interaction* (North–Holland, Amsterdam, 1976).

[27] F. Gross, *Relativistic Quantum Mechanics and Field Theory* (Wiley-Interscience, New York, 1993).

[28] F. Gross and D. O. Riska, Phys. Rev. C **36**, 1928 (1987).

[29] J. C. Ward, Phys. Rev. **78**, 182 (1950); Y. Takahashi, Nuovo Cimento **6**, 371 (1957).

[30] R. A. Arndt and L. D. Roper, Scattering Analysis and Interactive Dial-in (SAID) program, Virginia Polytechnic Institute and State University.

[31] S. Galster, H. Klein, J. Moritz, K. H. Schmidt, and D. Wegener, Nucl. Phys. **B32**, 221 (1971).

[32] H. Ito and F. Gross, Phys. Rev. Lett. **71**, 2555 (1993).

APPENDIX A

THE FIRST APPENDIX

This is where I put the text of the first appendix. A good place to put a mathematical derivation not neccessary to be in the thesis but still useful to have.

APPENDIX B

THE SECOND APPENDIX

This is where I put the text of the second appendix.

VITA

A. Student
Department of Physics
Old Dominion University
Norfolk, VA 23529

This is where I tell you about my academic background and list all of my accomplishments.

Typeset using LaTeX.